TENTH AUSTRALASIAN FLUID MECHANICS
CONFERENCE - UNIVERSITY OF MELBOURNE
11-15 DECEMBER 1989

NUMERICAL SOLUTION OF THE INCOMPRESSIBLE NAVIER-STOKES EQUATIONS FOR STEADY-STATE AND TIME-DEPENDENT PROBLEMS

Stuart E. ROGERS[1], Dochan KWAK[2] and Cetin KIRIS[3]

[1]Sterling Federal Systems, Palo Alto, California, USA

[2]NASA Ames Research Center, Moffett Field, California 94035, USA

[3]Stanford University, Stanford 94305, California, USA

ABSTRACT

An algorithm for the solution of the incompressible Navier-Stokes equations in three-dimensional generalized curvilinear coordinates is presented. The algorithm can be used to compute both steady-state and time-dependent flow problems. The algorithm is based on the method of artificial compressibility and uses a higher-order flux-difference splitting technique for the convective terms. Time accuracy is obtained in the numerical solutions by subiterating the equations in pseudo-time for each physical time step. The equations are solved with an unconditionally stable line-relaxation scheme. Computational results for the steady-state solution of flow through a square duct with a 90° bend and for flow through an artificial heart configuration with moving boundaries are presented.

INTRODUCTION

Numerical solutions to the incompressible Navier-Stokes equations are in greater demand than ever before as the field of computational fluid dynamics (CFD) increases its impact as an engineering tool. Problems which can be addressed by the incompressible Navier-Stokes equations include low-speed flows in aerodynamics, internal flows in propulsion, and even problems in biomedical fluid analysis. The more efficient a is, the more useful a tool it will be for analysis. Therefore, there is a continuing interest in finding solution methodologies which will produce results using the least amount of computing time. This is particularly true for unsteady, three-dimensional (3-D) problems. Time-accurate solutions of the incompressible Navier-Stokes equations are most time consuming because of the elliptical nature of the governing equations. A disturbance at one point in space affects the entire flow domain instantaneously. This requires that the numerical algorithm propagates information through the entire flow domain during one discrete time step.

The current work involves an extension of the two-dimensional (2-D) flow code developed by the Rogers et al. (1988) into 3-D. The algorithm is based on an artificial compressibility approach, which directly couples the pressure and velocity fields at the same time level, and produces a hyperbolic system of equations. This makes possible to use some of the upwind differencing schemes which have recently been developed for the compressible Euler and Navier-Stokes equations. Using the method of Roe (1981) the convective terms are differenced by an upwind method that is biased by the signs of the eigenvalues of the local flux Jacobian. In the current formulation the set of numerical equations are solved using a nonfactored line relaxation scheme.

In the following sections, the details of the artificial compressibility scheme and its use in solving the incompressible Navier-Stokes equations for steady-state and time-dependent problems are given. The upwind-differencing scheme is detailed, and then the implicit solution procedure is discussed. Computed results are presented for the flow through a curved square duct and for the unsteady flow through an artificial heart configuration with a moving boundary.

GOVERNING EQUATIONS

The governing equations for incompressible, constant density flow are written in conservative form in generalized coordinates as

$$\begin{aligned} &\frac{\partial \hat{u}}{\partial t} = -\frac{\partial}{\partial \xi}(\hat{e}-\hat{e}_v) - \frac{\partial}{\partial \eta}(\hat{f}-\hat{f}_v) - \frac{\partial}{\partial \zeta}(\hat{g}-\hat{g}_v) = -\hat{r} \\ &\frac{\partial}{\partial \xi}\left(\frac{U}{J}\right) + \frac{\partial}{\partial \eta}\left(\frac{V}{J}\right) + \frac{\partial}{\partial \zeta}\left(\frac{W}{J}\right) = 0 \end{aligned} \tag{1}$$

where $\hat{u}$ is the vector of the velocity components divided by J, $\hat{r}$ represents the right-hand side of the momentum equations, J is the Jacobian of the transformation, $\hat{e}, \hat{f}\hat{g}$ are the convective fluxes, $\hat{e}_v, \hat{f}_v, \hat{g}_v$ are the viscous fluxes, and U, V, W are the contravarient velocities.

STEADY-STATE FORMULATION

The artificial compressibility relation is introduced by adding a time derivative of pressure to the continuity equation

$$\frac{\partial p}{\partial \tau} = -\beta \nabla \cdot \hat{u} \tag{2}$$

where p is the pressure. In the steady-state formulation the equations are to be marched in a time-like fashion until the right-hand side $\hat{r}$ in Eq. (1) and the divergence of velocity converges to zero. The time variable for this process no longer represents physical time and so in the momentum equations t is replaced with τ, which can be thought of as a pseudo-time or iteration parameter. Combining Eq. (2) with the momentum equations gives the following system of equations

$$\frac{\partial \hat{D}}{\partial \tau} = -\frac{\partial}{\partial \xi}(\hat{E}-\hat{E}_v) - \frac{\partial}{\partial \eta}(\hat{F}-\hat{F}_v) - \frac{\partial}{\partial \zeta}(\hat{G}-\hat{G}_v) = -\hat{R} \tag{3}$$

where $\hat{R}$ is defined here as the residual vector of these equations and where

$$\hat{D} = \frac{1}{J}\begin{bmatrix} p \\ u \\ v \\ w \end{bmatrix}$$

$$\hat{E} = \begin{bmatrix} \beta U/J \\ \hat{e} \end{bmatrix} \quad \hat{F} = \begin{bmatrix} \beta V/J \\ \hat{f} \end{bmatrix} \quad \hat{G} = \begin{bmatrix} \beta W/J \\ \hat{f} \end{bmatrix} \qquad (4)$$

$$\hat{E}_v = \begin{bmatrix} 0 \\ \hat{e}_v \end{bmatrix} \quad \hat{F}_v = \begin{bmatrix} 0 \\ \hat{f}_v \end{bmatrix} \quad \hat{G}_v = \begin{bmatrix} 0 \\ \hat{g}_v \end{bmatrix}$$

The pseudo-time derivative is replaced by an implicit Euler finite-difference formula and the right-hand side is linearized resulting in

$$\left[\frac{1}{J\Delta\tau} I + \left(\frac{\partial \hat{R}}{\partial D}\right)^n\right](D^{n+1} - D^n) = -R^n \qquad (5)$$

where a superscript n denotes quantities at the nth pseudo-time iteration level and where I is a 4 x 4 identity matrix and where $D = J\hat{D}$. If this equation were solved exactly as it is, then for very large $\Delta\tau$ this would become a Newton iteration for a steady-state solution. However, it is not feasible to form the exact Jacobian of the residual vector R. Before these details are discussed, however, an equation similar to Eq. (6) for time-dependent problems will be developed.

TIME-ACCURATE FORMULATION

In the time-accurate formulation the time derivatives in the momentum equations are differenced using a second-order, three-point, backward-difference formula

$$\frac{3\hat{u}^{n+1} - 4\hat{u}^n + \hat{u}^{n-1}}{2\Delta t} = -\hat{r}^{n+1} \qquad (6)$$

where the superscript n denotes the quantities at time $t = n\Delta t$ and $\hat{r}$ is the right-hand side given in Eq. (1). To solve Eq. (7) for a divergence free velocity at the $n+1$ time level, a pseudo-time level is introduced and is denoted by a superscript m. The equations are iteratively solved such that $\hat{u}^{n+1,m+1}$ approaches the new velocity $\hat{u}^{n+1}$ as the divergence of $\hat{u}^{n+1,m+1}$ approaches zero. To drive the divergence of this velocity to zero, the following artificial compressibility relation is introduced:

$$\frac{p^{n+1,m+1} - p^{n+1,m+1}}{\Delta\tau} = -\beta\nabla\cdot\hat{u}^{n+1,m+1} \qquad (7)$$

where τ denotes pseudo-time and β is an artificial compressibility parameter. In this form it can be seen that the constants β and $\Delta\tau$ are not independent. However, they are kept separate here primarily because of the following reason. In the numerical equation which approximates the previous partial differential equation, the change in pressure becomes a nonlinear function of β because of the use of upwind differencing. Therefore, in the numerical equation, β and $\Delta\tau$ become independent.

Combining Eq. (7) with the momentum equations and linearizing gives the following equation in delta form

$$\left[\frac{I_{t\tau}}{J} + \left(\frac{\partial \hat{R}}{\partial D}\right)^{n+1,m}\right](D^{n+1,m+1} - D^{n+1,m}) = -\hat{R}^{n+1,m} - \frac{I_m}{\Delta t}(1.5\hat{D}^{n+1,m} - 2\hat{D}^n + 0.5\hat{D}^{n-1}) \qquad (8)$$

where

$$I_{t\tau} = \text{diag}\left[\frac{1}{\Delta\tau}, \frac{1.5}{\Delta t}, \frac{1.5}{\Delta t}, \frac{1.5}{\Delta t}\right] \qquad I_m = \text{diag}[0,\ 1,\ 1,\ 1]$$

As can be seen, Eq. (8) is very similar to the steady-state formulation given by Eq. (5). In a sense the time-accurate formulation requires the solution of a steady-state problem in order to advance one physical time step. Both systems of equations will require the discretization of the same residual vector $\hat{R}$. The derivatives of the viscous fluxes in this vector are approximated using second-order central differences. The formation of the convective fluxes is not such a simple matter and is the subject of the next section.

UPWIND DIFFERENCING

Upwind differencing is used to numerically compute the convective flux derivatives. Flux-difference splitting is used here to structure the differencing stencil based on the sign of the eigenvalues of the convective flux Jacobian. The scheme presented here was originally derived by Roe (1981) as an approximate Riemann solver for the compressible gas dynamics equations.

The derivative of the convective flux in the ξ direction is approximated by

$$\frac{\partial \hat{E}}{\partial \xi} \approx \frac{[\tilde{E}_{i+1/2} - \tilde{E}_{i-1/2}]}{\Delta\xi} \qquad (9)$$

where $\tilde{E}_{i+1/2}$ is a numerical flux and i is the discrete spatial index for the ξ direction.

The numerical flux is given by

$$\tilde{E}_{i+1/2} = \frac{1}{2}\left[\hat{E}(D_{i+1}) + \hat{E}(D_i) - \phi_{i+1/2}\right] \qquad (10)$$

where the $\phi_{i+1/2}$ is a dissipation term. For $\phi_{i+1/2} = 0$ this represents a second-order central difference scheme. A first-order upwind scheme is given by

$$\phi_{i+1/2} = \left(\Delta E^+_{i+1/2} - \Delta E^-_{i+1/2}\right) \qquad (11)$$

a third-order scheme is given by

$$\phi_{i+1/2} = -\frac{1}{3}\left(\Delta E^+_{i-1/2} - \Delta E^+_{i+1/2} + \Delta E^-_{i+1/2} - \Delta E^-_{i+3/2}\right) \qquad (12)$$

where $\Delta E^{\pm}$ is the flux difference across positive or negative traveling waves. This is computed as

$$\Delta E^{\pm}_{i+1/2} = A^{\pm}(\bar{D})\Delta D_{i+1/2} \qquad (13)$$

where the Δ operator is given by

$$\Delta D_{i+1/2} = D_{i+1} - D_i$$

The plus (minus) Jacobian matrix has only positive (negative) eigenvalues and is computed from

$$A^{\pm} = X_1\Lambda_1^{\pm}X_1^{-1} \qquad \Lambda_1^{\pm} = \frac{1}{2}(\Lambda_1 \pm |\Lambda_1|) \qquad (14)$$

where the subscript 1 denotes matrices corresponding to the ξ-direction flux. The matrices X_1 and X_1^{-1} are the right and left eigenvectors of the Jacobian matrix of the flux vector, and Λ_1 is a diagonal matrix consisting of its eigenvalues. All matrices appearing in the upwind dissipation term must be evaluated at a half point (denoted by i+1/2). To do this a special averaging of the dependent variables at neighboring points must be performed. The Roe (1981) properties which are necessary for a conservative scheme, are satisfied if the following averaging procedure is employed

$$\bar{D} = \frac{1}{2}(D_{i+1} + D_i) \qquad (15)$$

IMPLICIT SCHEME

The Eqs. (5) and (8) are numerically represented and solved using a Gauss-Seidal line-relaxation scheme similar to the one used by MacCormack (1985) and Chakravarthy (1984). Approximate Jacobians of the residual vector resulting from first-order upwind-differenced fluxes are substituted for the $\frac{\partial R}{\partial D}$ term on the left-hand side. Instead of factoring this banded matrix, it is approximately solved using a line-relaxation. Using this, a sweep direction is chosen and all terms on the left hand side from points off this sweep line are multiplied by the latest known ΔD and moved to the right-hand side. The resulting set of equations is a tridiagonal system of 4 x 4 blocks. This system is solved is for each line as the domain is swept several times.

COMPUTED RESULTS

Presented here are the results of two different laminar flow computations. These are the flow through a square duct with a 90° bend, and the flow through an artificial heart. The computing times reported here are the CPU seconds used on a Cray 2. For these problems it was found that the implicit scheme remained unconditionally stable, and so all of the $1/\Delta\tau$ terms were set to zero.

Square Duct With 90° Bend

The flow through a square duct with a 90° bend was used as a steady-state test case. This particular geometry was studied experimentally by Humphrey et al (1977) which enables comparisons to be made with the current computed results. Four different grids were used whose dimensions are 31 x 11 x 11, 41 x 21 x 21, 51 x 31 x 31, and 61 x 41 x 41. The problem was non-dimensionalized using the side of the square cross-section as the unit length, and the average inflow velocity as the unit velocity. The Reynolds number was 790 and β was set to one. The straight inflow section before the bend was set to a length of five as was the outflow section downstream of the bend. The radius of curvature of the inner wall in the curved section was 1.8 units in length. The inflow velocity profile was prescribed to be that of a fully developed laminar straight square duct as given by White (1974).

The convergence for all four grid cases is nearly identical. The maximum residual drops to machine zero in less than 300 iterations for all cases. The solution is considered converged if the maximum residual has converged at least four orders of magnitude. This is is obtained in less than 115 iterations for all four cases. The computing time required to obtain a converged solution for each of the four cases are 32, 196, 550, and 1067 sec, respectively. The computed results are compared to the experimental results of Humphrey et al. (1977) in Fig. 1. Shown are the longitudinal velocity profiles at various streamwise stations for two different cross-flow locations. In Fig. 1a, the velocity profiles are taken at z=0.25, that is half way between the x-y plane wall and the x-y symmetry plane. The second location, shown in Fig. 2b, is from the x-y plane at z=0.5, or the x-y symmetry plane. In each of these figures, the profiles are shown at x=0 (the inflow boundary), at x=2.5 and at four positions in the curved section corresponding an angle of 0, 30, 60, and 90.° The symbols represent the experimental results and the lines represent the computed solutions. The computations for the two finest grid cases are seen to be in very good agreement with each other, indicating that these represent a grid-independent solution. Good comparison is seen between the computation and the experiment.

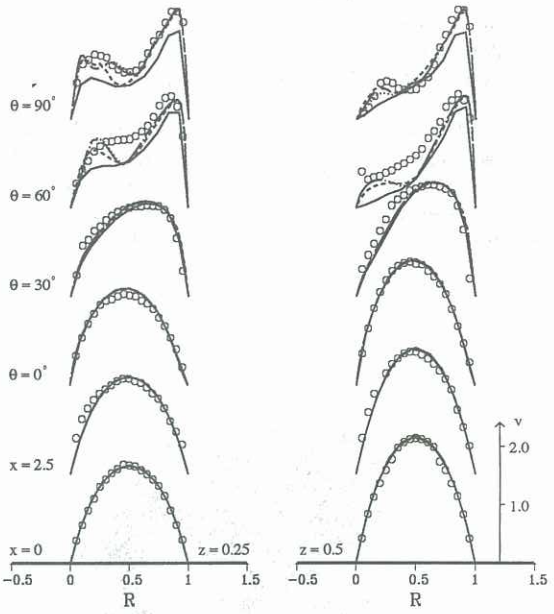

Fig. 1 Streamwise-velocity profiles at x=0, x=2.5, θ = 0°, θ = 30°, θ = 60°, θ = 90°. Solid line = 31x11x11 grid, dash line = 41x21x21 grid, dotted line = 51x31x31 grid, chain-dot line = 61x41x41 grid, and o = experiment.

Artificial Heart Flow

The present flow solver has been used to compute the flow inside an artificial heart which was designed by Penn State University and has been studied experimentally by Tarbell et al. (1986). The purpose of the current calculations is to demonstrate and analyze the present capability to compute a time-accurate incompressible flow through a complex internal device with moving-boundaries.

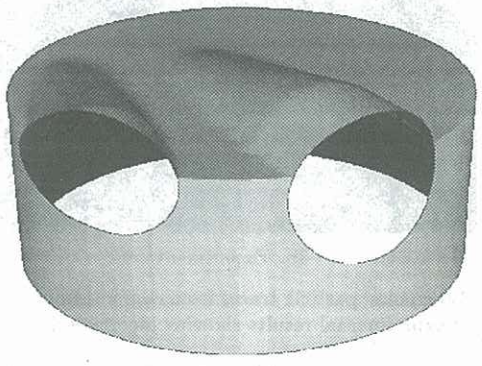

Outflow Valve Inflow Valve

Fig. 2 Artificial-heart geometry showing valve openings.

The geometry used for the current model is depicted in Fig. 2. The heart is composed of a cylindrical chamber with two openings on the side for valves. The pumping action is provided by a piston surface which moves up and down inside the chamber. The diameter of the piston is 7.4 cm, with a stroke length of 2.54 cm. The problem was nondimensionalized with a unit length of 2.54 cm and a unit velocity of 40 cm/sec. The actual artificial heart has cylindrical tubes containing tilting flat disk valves extending out of each of the side valve openings. In the computational model these valves are not modeled, instead the boundary conditions at

the side openings are specified to instantaneously open and close at the right moment. This simplification allows a single zone to be used to model the flow inside the chamber. The flow is assumed laminar, and the Reynolds number based on the the unit length and velocity is set to 100. In the actual heart the Reynolds number is about 600, and regions of the flow are turbulent. The fluid is also assumed to be Newtonian. This corresponds to the experiment of Tarbell et al. (1986) who used a water and glycerin fluid whose viscosity is nearly the same as blood, about 3.5 centipoise, but unlike blood exhibits Newtonian fluid behavior.

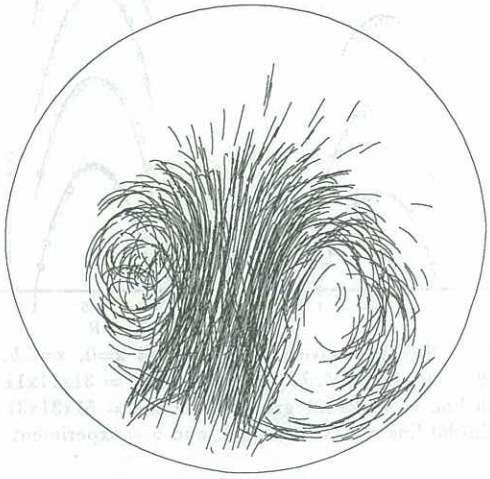

3a. Computation

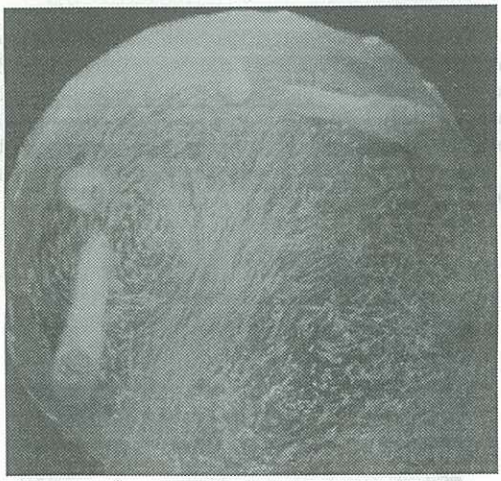

3b. Experiment

Fig. 3 Incoming particle traces from computations and picture of experimental results showing incoming fluid.

Inside the heart an H-H grid topology with dimensions of 39 x 39 x 51 is used. The surface grid was generated using a biharmonic grid generator over several sections. The interior points were filled using an algebraic solver coupled with an elliptic smoother. As the piston moved up and down inside the chamber, the grid points below the valve openings were compressed and expanded, respectively. Thus a new grid was generated at each time step.

The flow was computed using a time step Δt of 0.025, and a β of 500. The piston moved with a constant nondimensionalized velocity of ± 0.2 between it's top and bottom positions, requiring 200 physical time steps for one period of the piston's motion. During each time step, the subiterations were carried out until the maximum residual converged dropped below 10^{-3} or until a maximum of 20 subiterations were used. During most of the piston's cycle only 12-15 subiterations were required, but when the piston was changing directions, it did not completely converge in 20 subiterations. The computing time required for each period of the piston's motion was approximately four hr. The computations were run for four periods during which time particle paths were computed after being released near the inflow valve.

Figure 3a shows some computed particle traces as the piston nears it's bottom position. Two distinct vortices are seen to have formed from the flow separating as it enters the chamber. Figure 3b shows an experimental photograph (J. M. Tarbell: private communication, 1988) of bubbles entering the chamber as the piston nears it's bottom position. A similar two-vortex system is seen to form.

CONCLUSION

An algorithm for computing steady-state and time-varying solutions of the incompressible Navier-Stokes equations has been presented. The method of artificial compressibility allows the equations to be solved as a hyperbolic system in pseudo-time. This requires the solution of a steady-state problem at each physical time step for the time-accurate formulation. The use of upwind differencing makes the system of numerical equations diagonally dominant. With the use of a nonfactored implicit line-relaxation scheme, the code can be run at very large time steps, and very fast convergence is seen. The results showed good comparison with experiment for the flow through a square duct. The computations of the flow through an artificial heart shows the capability of the code to simulate complicated internal flows with moving boundaries within a reasonable amount of computing time. Further advances in the convergence speed of the algorithm will still be very helpful in increasing the usefulness of this code as a design tool.

REFERENCES

CHAKRAVARTHY, S. R. (1984) "Relaxation methods for unfactored implicit upwind schemes. AIAA Paper 84-0165.

HUMPHREY, J. A. C., TAYLOR, A. M. K., and WHITELAW, J. H. (1977) Laminar Flow in a square duct of strong curvature. J. Fluid Mech., 83, part 3, pp. 509–527.

MACCORMACK, R. W. (1985) Current status of numerical solutions of the Navier-Stokes equations. AIAA Paper 85-0032.

RAI, M. M. (1987) Navier-Stokes simulations of blade-vortex interaction using high-order accurate upwind schemes. AIAA Paper 87-0543.

ROE, P. L. (1981) Approximate riemann solvers, parameter vectors, and difference schemes. J. Comput. Phys. 43, p. 357.

ROGERS, S. E. and KWAK, D. (1988) An upwind differencing scheme for the time-accurate incompressible Navier-Stokes equations. AIAA Paper 88-2583, to be published in the AIAA J.

TARBELL, J. M., GUNSHINAN, J. P., GESELOWITZ, D. B., ROSENBURG, G., SHUNG, K. K., and PIERCE, W. S. (1986) Pulse ultrasonic doppler velocity measurements inside a left ventricular assist device. J. Biomech. Engr., Trans. ASME, 108, pp. 232–238.

WHITE, F. M., (1974) Viscous Fluid Flow, McGraw-Hill, New York, p. 123.